Optica Applicata, Vol. LIII, No. 2, 2023
DOI: 10.37190/oa230211

Propagation properties of partially coherent array beams with a non-uniform polarization

XIANYANG YANG[1], WENYU FU[2,*]

[1]School of Intelligent Manufacturing and Energy Engineering,
Jiang-Xi University of Engineering Xinyu,
338000, Jiangxi, China

[2]College of Science, Jiang-Xi University of Engineering Xinyu,
338000, Jiangxi, China

[*]Corresponding author: qytcfwy@163.com

We study a new class of partially coherent array beams with a non-uniform polarization, named radially polarized Gaussian Schell-model array (RPGSMA) beams and analyze the reliability conditions for the array beams based on the unified theory of coherence and polarization, Moreover, the statistical properties of such beam propagating in free space are investigated in detail. It is found that, the propagation properties of the RPGSMA beams are closely related to initial beam parameters. With an appropriate choice of the beam parameters, the average intensity will evolve into optical lattice patterns, and the degree of coherence (DOC) from the lattice distribution on the original plane evolves into a Gaussian profile in the far field, and the degree of polarization (DOP) appears a periodical grid-like distribution on propagation. These results may be beneficial to particle trapping and free-space optical communications.

Keywords: partially coherent, radially polarization, Gaussian Schell-model array beams, propagation properties.

1. Introduction

In recent years, due to their wide application in many fields, array beams with spatial periods have received more and more attention [1–4]. Compared with a single beam, coherent array beams with smaller source size divergence can produce higher output power and lattice-like intensity distribution [5]. In order to obtain array beams, researchers have used theoretical and experimental methods to generate various types of array beams [6], such as Gaussian Schell-model array beam [7], partially coherent flat-topped laser array [8], various partially coherent partially phase-locked laser array [9, 10], partially coherent Hermite–Gaussian linear array beam [11], partially coherent vortex beam array [12], *etc*.

Apart from such studies dedicated to scale array beams, there has been substantial interest in studying the stochastic electromagnetic beams attributing to their importance in optical coherence theory and in practical applications [13, 14]. Since the unified theory of coherence and polarization was formulated by WOLF [15], a lot of work has been done on the propagation of stochastic electromagnetic beams in different optical systems or media. In general, due to the difference in the correlation coefficient between the x and y components of the electric field vector at the two source points, the polarization characteristics of the beam may change during propagation, and random medium can also cause the polarized properties of beams to change on propagation [16]. Recently, a few of papers have appeared on electromagnetic twisted Gaussian Schell -model array beams [17]. It was demonstrated that the twist strength has significant influence on the degree of polarization of electromagnetic Gaussian Schell-model array beams on propagation.

On the other hand, the polarization properties of various laser beams also attracted much attention. Unlike uniformly polarized beam such linearly or elliptically polarized beam, radially polarized beam as a typical case of cylindrical vector beam with non-uniform state of polarization, exhibits many unique properties [18], and has been used in many fields [19–21].

In this paper, as extension of vector partially coherent beams, we introduce a new kind of partially coherent vector array beams and discuss the reliability conditions. Furthermore, based on the extended Huygens–Fresnel integral, we also derive the analytical expressions for the elements of the cross-spectral density matrix of such beams propagating in free space and investigate the statistical properties of a radially polarized CGCSM beam on propagation in detail, and some interesting results are found.

2. Radially polarized Gaussian Schell-model array sources

The elements of cross-spectral density (CSD) matrix that characterizes second-order correlation properties of a statistical source at a pair of point r_1 and r_2 in the source plane $z = 0$ are given by the formula [22]

$$W_{\alpha\beta}(r_1, r_2) = \langle E_\alpha^*(r_1) E_\beta(r_2) \rangle, \qquad \alpha, \beta = x, y \tag{1}$$

where E_x and E_y are the components of the electric vector perpendicular to the direction of the asterisk which denotes the complex conjugate and the angular brackets which denote a monochromatic ensemble average.

To be a mathematically genuine and physically realizable correlation function, the CSD matrix of RPHNUCA beams needs to satisfy the non-negative definiteness condition.

$$W_{\alpha\beta}(r_1, r_2) = \int p_{\alpha\beta}(v) H_\alpha^*(r_1, v) H_\beta(r_2, v) \, \mathrm{d}v \tag{2}$$

where $p_{\alpha\beta}(v)$ is a non-negative weight function, $H_\alpha(r_1, v)$ and $H_\beta(r_2, v)$ are two arbitrary kernels. They have a variety of choices and each choice is likely to lead to distinct

classes of CSD matrices. According to Ref. [22,23], for the beam sources to display radial polarization, we can set the kernel as follows:

$$H_\alpha(r, v) = \frac{\alpha}{w_0} A_\alpha \exp\left(\frac{|r|}{w_0^2}\right) \exp(-2\pi \mathrm{i} v r) \tag{3}$$

here v denotes a two-dimensional vector, A_x and A_y are the amplitudes of x and y components of the electric field, respectively, and we assume $A_x = A_y = 1$, w_0 is the beam width of the source. To obtain a Gaussian array with $N \times M$ profile in the far field, we select the following form of the weight function $p_{\alpha\beta}(v)$ [5]

$$\begin{aligned} p_{\alpha\beta}(v) = {} & \frac{2\pi\delta_{\alpha\beta}^2}{NM} B_{\alpha\beta} \exp\left[-2\pi(\delta_{\alpha\beta}^2 v_x^2 + \delta_{\alpha\beta}^2 v_y^2)\right] \\ & \times \sum_{n=-P}^{P} \cosh(4\pi^2 \delta_{\alpha\beta} n R_x v_x) \exp(-2\pi^2 n^2 R_x^2) \\ & \times \sum_{m=-Q}^{Q} \cosh(4\pi^2 \delta_{\alpha\beta} m R_y v_y) \exp(-2\pi^2 m^2 R_y^2) \end{aligned} \tag{4}$$

where v_x and v_y are two components of vector v, $P = (N-1)/2$, $Q = (M-1)/2$. The parameters R_x, R_y, δ_{xx}, δ_{yy} and δ_{xy} are the positive real constants, and the parameters δ_{xx}, δ_{yy} and δ_{xy} denote widths of auto-correlation functions of x component of the field, of the y component of the field, and of the mutual correlation function of x and y field components, respectively, and $\delta_{xy} = \delta_{yx}$. The complex correlation coefficient $B_{xy} = |B_{xy}| \exp(\mathrm{i}\varphi)$ and $B_{xy} = B_{yx}^*$. The function $\cosh(\cdot)$ is the hyperbolic cosine function. In addition, one can clearly see from Eq. (2) that $p_{\alpha\beta}(v)$ is non-negative for any values. Upon substituting from Eqs. (3) and (4) into Eq. (2), after some straight forward calculation, one can express the spectral DOC function as follows

$$\begin{aligned} W_{\alpha\beta}^{(0)}(\mathrm{r}_1, \mathrm{r}_2, 0) = {} & \frac{1}{NM} \frac{\alpha\beta}{w_0^2} A_\alpha A_\beta B_{\alpha\beta} \exp\left(\frac{|\mathrm{r}_1| + |\mathrm{r}_2|}{4w_0^2}\right) \exp\left[\frac{-(x_1 - x_2)^2}{2\delta_{\alpha\beta}^2}\right] \\ & \times \exp\left[\frac{-(y_1 - y_2)^2}{2\delta_{\alpha\beta}^2}\right] \sum_{n=-P}^{P} \cos\left[C_x(x_1 - x_2)\right] \sum_{m=-Q}^{Q} \cos\left[C_y(y_1 - y_2)\right] \end{aligned} \tag{5}$$

where $C_x = 2\pi n R_x / \delta_{\alpha\beta}$, and $C_y = 2\pi m R_y / \delta_{\alpha\beta}$. The random sources whose CSD matrix is Eq. (5) may be termed as radially polarized Gaussian Schell-model array (RPGSMA) sources.

Now, let's analyze the reliability of RPHNUCA beam source. First, to guarantee the physically realizable field described in Eq. (5), it is necessary to establish the restrictions for the source parameters

Thus, the CSD matrix must be quasi-Hermitian [15], *i.e.*, $W_{\alpha\beta}(r_1, r_2) = W_{\beta\alpha}(r_1, r_2)$. Second, the genuine CSD matrices of the beam must satisfy the non-negative conditions given in [24]. Finally, as a radially polarized beam, the beam is linearly polarized at any point in the source plane, indicating that the minor semi-axes of the polarization ellipse equal to zero, and the polarization orientation angle at any point should satisfy $\theta(x, y) = \arctan(y/x)$. The state of polarization (SOP) of a beam can be characterized by a polarization ellipse. In order to satisfy the above conditions, our RPHNUCA beams must additionally satisfy $B_{xy} = B_{yx} = 1$ and $\delta_{xx} = \delta_{yy} = \delta_{yx} = \delta$, therefore, the CSD elements of the RPGSMA sources become

$$W_{\alpha\beta}^{(0)}(r_1, r_2) = \frac{1}{NM}\frac{\alpha\beta}{w_0^2}B_{\alpha\beta}\exp\left(\frac{|r_1^2| + |r_2^2|}{4w_0^2}\right)\exp\left[\frac{-(x_1 - x_2)^2}{2\delta_0^2}\right] \times \exp\left[\frac{-(y_1 - y_2)^2}{2\delta_0^2}\right]\sum_{n=-P}^{P}\cos\left[C_x(x_1 - x_2)\right]\sum_{m=-Q}^{Q}\cos\left[C_y(y_1 - y_2)\right] \tag{6}$$

3. Cross-spectral density of the RPGSMA beams propagating in free space

Suppose that the source in Eq. (6) generates a beam-like field propagating from the source plane $z = 0$) into the half space $z > 0$. According to the extended Huygens –Fresnel principle, the elements of the cross-spectral density matrix at two positions $r_1 = (\rho_1, z)$ and $r_2 = (\rho_2, z)$ in any transverse plane are related to those in the source plane as [24]

$$W_{\alpha\beta}(\rho_1, \rho_2, z) = \iint W_{\alpha\beta}^{(0)}(r_1, r_2)\,\zeta^*(\rho_1, r_1, z)\,\zeta(\rho_2, r_2, z)\,\mathrm{d}r_1\,\mathrm{d}r_2 \tag{7}$$

where $\zeta(\rho, r, z)$ is a free-space Green's function:

$$\zeta(\rho, r, z) = \frac{-\mathrm{i}k\exp(\mathrm{i}kz)}{2\pi z}\exp\left[\frac{\mathrm{i}k}{2\pi z}(\rho - r)^2\right] \tag{8}$$

By substituting Eqs. (6) and (8) into Eq. (7) and performing mathematical calculation, we finally obtain the following expression for each element of the cross-spectral density matrix of a RPGSMA beam in free space

$$W_{xx}(\rho_1, \rho_2, z) = \frac{\pi^2}{16\lambda^2 z^2 w_0^2 a^2 b^2} \exp\left[\frac{-\mathrm{i}k(\rho_1^2 - \rho_2^2)}{2z}\right] \times \sum_{n_x=-P}^{P} \sum_{n_y=-Q}^{Q} \sum_{\substack{i=\pm \\ j=\pm}} Q_{X_i, Y_j} \exp\left(\frac{X_{1i}^2 + Y_{1j}^2}{4a} + \frac{F_{X_i}^2 + F_{Y_j}^2}{4b}\right) \tag{9}$$

$$W_{xy}(\rho_1, \rho_2, z) = \frac{\pi^2 B_{xy}}{16\lambda^2 z^2 w_0^2 a^2 b^2} \exp\left[\frac{-\mathrm{i}k(\rho_1^2 - \rho_2^2)}{2z}\right] \times \sum_{n_x=-P}^{P} \sum_{n_y=-Q}^{Q} \sum_{\substack{i=\pm \\ j=\pm}} R_{X_i, Y_j} \exp\left(\frac{X_{1i}^2 + Y_{1j}^2}{4a} + \frac{F_{X_i}^2 + F_{Y_j}^2}{4b}\right) \tag{10}$$

$$W_{yy}(\rho_1, \rho_2, z) = \frac{\pi^2}{16\lambda^2 z^2 w_0^2 a^2 b^2} \exp\left[\frac{-\mathrm{i}k(\rho_1^2 - \rho_2^2)}{2z} + M(\rho_1 - \rho_2)^2\right] \times \sum_{n_x=-P}^{P} \sum_{n_y=-Q}^{Q} \sum_{\substack{i=\pm \\ j=\pm}} Q_{Y_j, X_i} \exp\left(\frac{X_{1i}^2 + Y_{1j}^2}{4a} + \frac{F_{X_i}^2 + F_{Y_j}^2}{4b}\right) \tag{11}$$

with

$$B_{\alpha\beta} = 1, \quad (\alpha, \beta = x, y) \tag{12a}$$

$$X_{1\pm} = \frac{\mathrm{i}}{2}\left(\frac{k x_1'}{z} \pm C_1\right), \quad X_{2\pm} = \frac{\mathrm{i}}{2}\left(\frac{k x_2'}{z} \pm C_1\right) \tag{12b}$$

$$Y_{1\pm} = \frac{\mathrm{i}}{2}\left(\frac{k y_1'}{z} \pm C_2\right), \quad Y_{2\pm} = \frac{\mathrm{i}}{2}\left(\frac{k y_2'}{z} \pm C_2\right), \tag{12c}$$

$$F_{X\pm} = X_{2\pm} - \frac{X_{1\pm}}{a\delta_0^2}, \quad F_{Y\pm} = Y_{2\pm} - \frac{Y_{1\pm}}{a\delta_0^2} \tag{12d}$$

$$a = \frac{1}{4w_0^2} + \frac{1}{2\delta_0^2} + \frac{\mathrm{i}k}{2z}, \qquad b = a^* - \frac{1}{4a\delta_0^2} \tag{12e}$$

$$Q_{X_\pm, Y_\pm} = \frac{1}{\delta_0^2} + F_{X\pm}\left(X_{1\pm} + \frac{F_{X\pm}}{2\delta_0^2}\right) \tag{12f}$$

$$Q_{Y_\pm, X_\pm} = \frac{1}{\delta_0^2} + F_{Y\pm}\left(Y_{1\pm} + \frac{F_{Y\pm}}{2\delta_0^2}\right) \tag{12g}$$

$$R_{X_\pm, Y_\pm} = \frac{1}{2b}\left(X_{1\pm} + \frac{F_{X\pm}}{2b\delta_0^2}\right)\left(Y_{2\pm} - \frac{Y_{1\pm}}{2a\delta_0^2}\right) \tag{12h}$$

Equations (9)–(11) can be considered as a general analytical expression of the CSD of the beam generated by a RPGSMA source. When $N_1 = N_2 = 1$, it would reduce to the propagated CSD for a RPGSMA beam. Applying Eqs. (13)–(16), one is ready to study the statistical properties of such a RPGSMA beam on propagation. Setting $\rho_1 = \rho_2 = \rho$, average intensity for a RPGSMA beam propagating in free space can be expressed as [18, 19]

$$S(\rho, z) = \mathrm{Tr}(\rho, \rho, z) = W_{xx}(\rho, \rho, z) + W_{yy}(\rho, \rho, z) \tag{13}$$

and the DOP of the beam can be calculated by the expression

$$P(\rho, z) = \sqrt{1 - \frac{4\,\mathrm{Det}\,W(\rho, \rho, z)}{\mathrm{Tr}\,W(\rho, \rho, z)}} \tag{14}$$

where $\mathrm{Det}\,W(\rho, \rho, z)$ and $\mathrm{Tr}\,W(\rho, \rho, z)$ denote the determinant and the trace, respectively. And the DOC for the beam at a pair of field points ρ_1 and ρ_2 can be written as

$$\mu(\rho_1, \rho_2, z) = \frac{\mathrm{Tr}\,W(\rho_1, \rho_2, z)}{\sqrt{\mathrm{Tr}\,W(\rho_1, \rho_1, z)}\,\sqrt{\mathrm{Tr}\,W(\rho_2, \rho_2, z)}} \tag{15}$$

4. Numerical results and discussions

In this section, we will demonstrate the evolution of statistical properties of a RPGSMA beam on propagation in free space. If no other explanation is made, those parameters are invariable in the following simulation: $\lambda = 632.8$ nm, $R_1 = 2R_2 = 3$ mm, $N_1 = N_2 = 2$. Figure 1 shows the evolution of the normalized spectral density $S/S_{\max}^{(0)}$ and its components $S_x/S_{x\max}^{(0)}$ along x direction and $S_y/S_{y\max}^{(0)}$ along y direction for a RPGSMA beam at several propagation distances in free space. It is clearly seen from the figure that profile of a RPGSMA beam is composed of two mutually perpen-

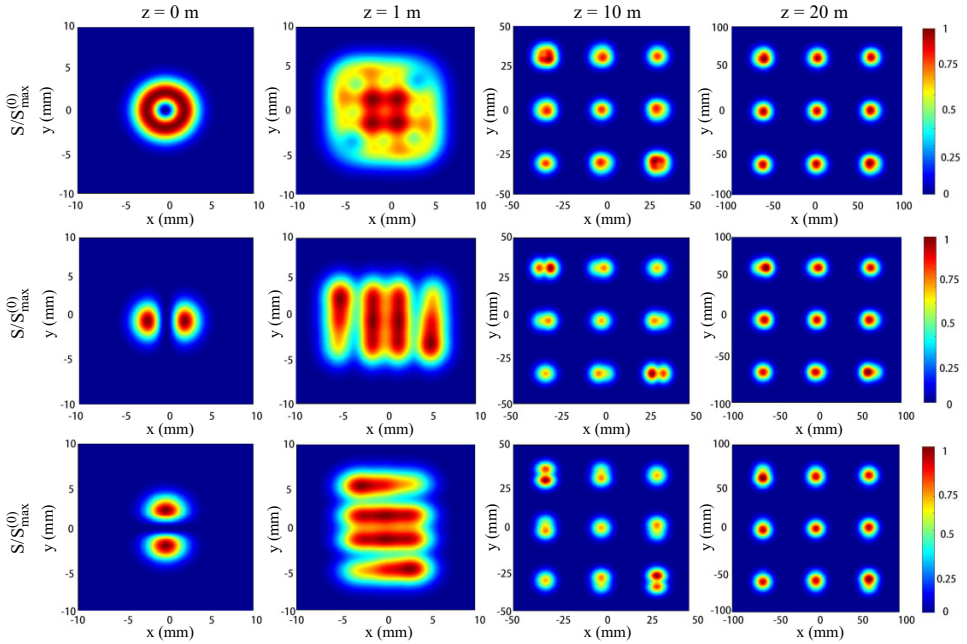

Fig. 1. The normalized spectral intensity of the RPGSMA beam at several propagation distances in free space with beam parameters $w_0 = 1.5$ mm and $\delta_0 = 0.3$ mm.

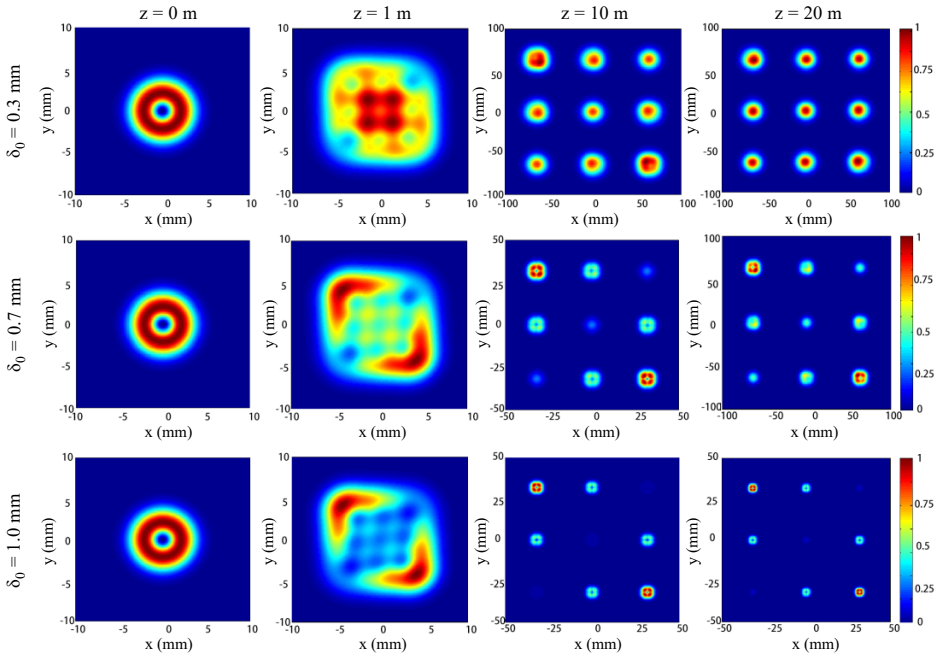

Fig. 2. The normalized spectral intensity of the RPGSMA beam at several propagation distances for different values of beam width δ_0 in free space and coherence length is chosen $w_0 = 1.5$ mm.

dicular beam components, which is dark hollow at the source plane, then gradually splits into arrays, and finally becomes a lattice-like uniform intensity distribution in the far zone.

In Figure 2, we presented evolution of the normalized spectral intensity of the RPGSMA beam at several propagation distances for different values of coherence length δ_0 in free space. One can see that the beam profile is dark hollow. As propagation distance increases, the spectral gradually evolved array beam, and the intensity distribution of the array beam varies with the coherence length. Furthermore, with the increase of the coherence length, the array energy moves to beam lobes along main diagonal direction, and the beam lobes on the sub-diagonal gradually weaken until they disappear. Figure 3 shows evolution of the normalized spectral intensity of the RPGSMA beam at several propagation distances for different values of beam width w_0 in free space. It can be found that the intensity distribution of the array beam is closely related to the beam width. The larger the beam width, the more uniform the intensity distribution of the array beam in the far field.

Next, we will turn to the analysis of the DOC change for the RPGSMA beam. In Fig. 4, we calculated variation of modulus of the DOC for a RPGSMA beam with different values of w_0 at several propagation distances. One can see that the DOC of the RPGSMA beam exhibits lattice-like distribution with circular symmetry in the original plane. With the increase of the beam width, the shape of the DOC evolves from doughnut profile into a Gaussian profile on propagation, and the larger the beam width, the

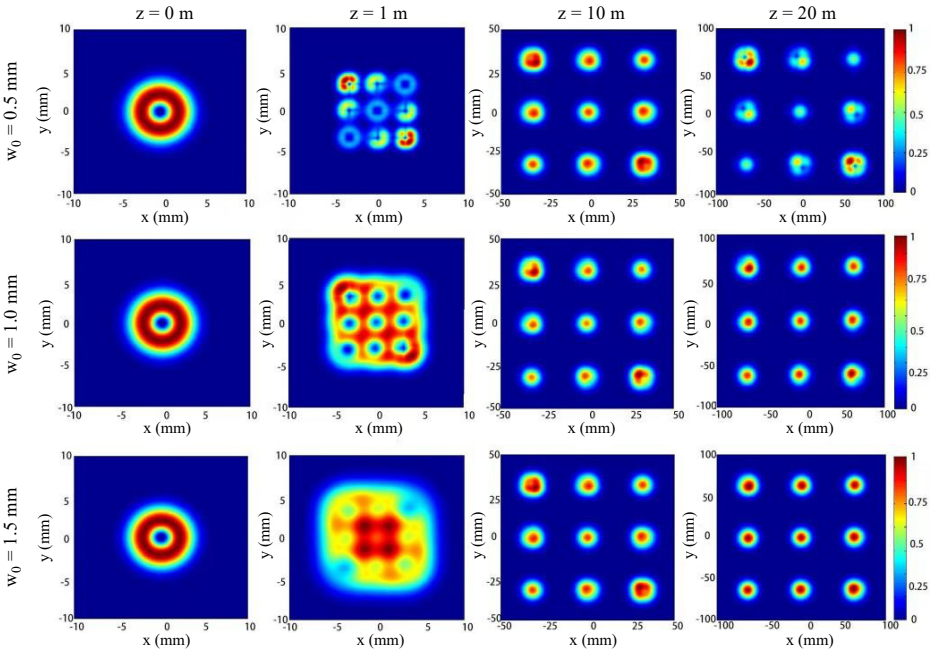

Fig. 3. The normalized spectral intensity of the RPGSMA beam at several propagation distances for different values of beam width w_0 in free space, and coherence length is chosen $\delta_0 = 0.3$ mm.

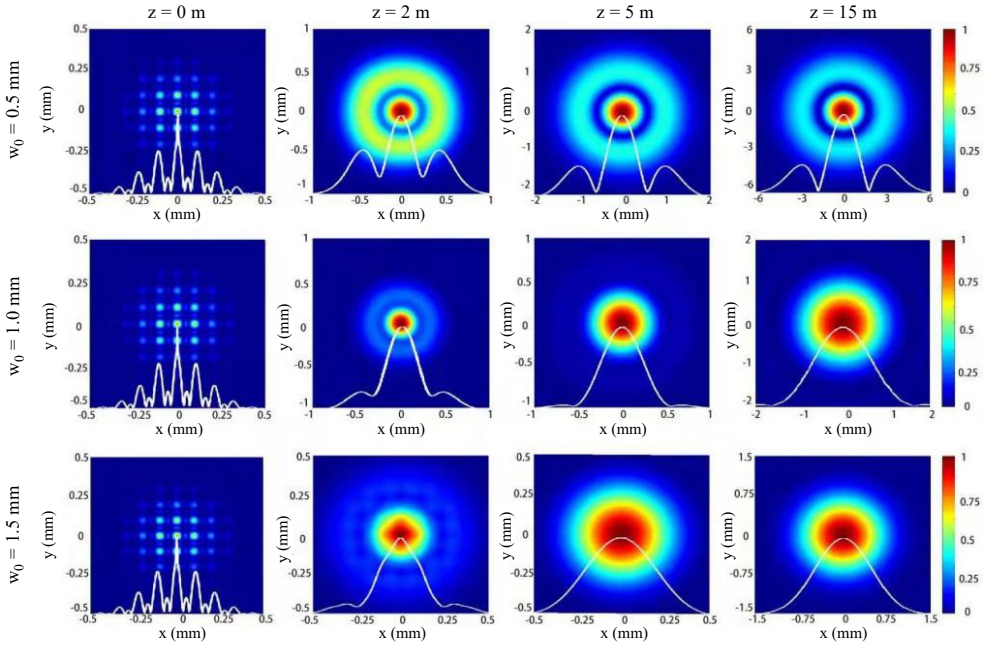

Fig. 4. Variation of modulus of the DOC at several propagation distances for different values of beam width w_0 in free space, and coherence length is chosen $\delta_0 = 0.3$ mm.

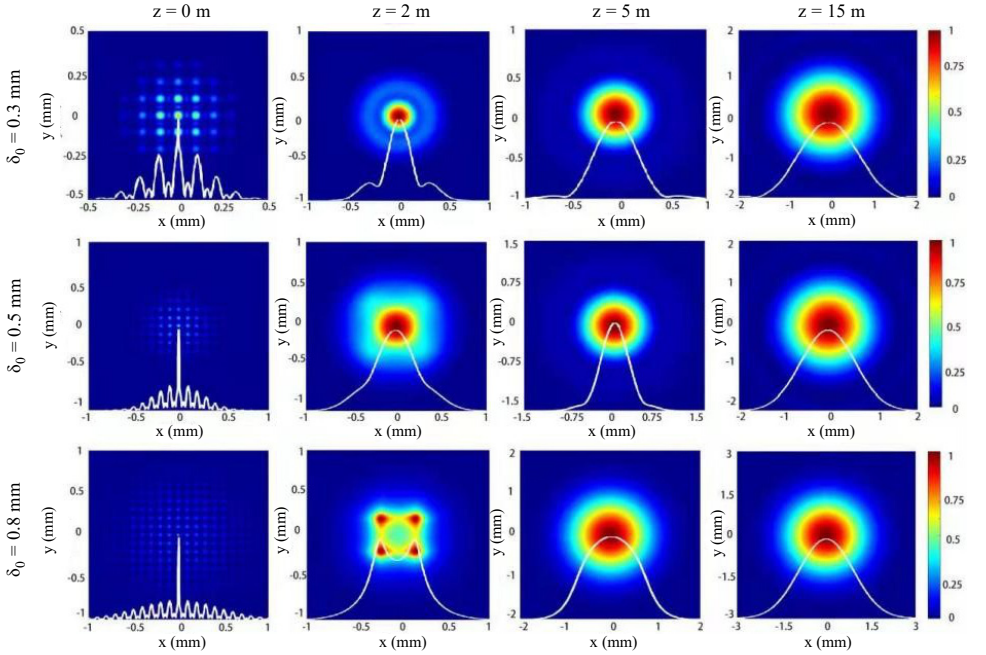

Fig. 5. Variation of modulus of the DOC at several propagation distances for different values of coherence length in free space, and beam width $w_0 = 1$ mm.

easier it is to form the Gaussian distribution, which are quite different from those of a single radially polarized beam.

Figure 5 illustrates variation of modulus of the DOC for a RPGSMA beam at several propagation distances for different values of coherence length in free space. One can find from the figures that the coherence length plays an important role in the DOC distribution of a RPGSMA beam. In the source plane, as the coherence length increases, the DOC values of the RPGSMA beam gradually decreases and its scales gradually expand. As the propagation distance increases, the DOC distribution of the RPGSMA beam progressively evolves, and also tends to a Gaussian distribution in the far field. Finally, we discuss the polarization properties of the RPGSMA beam. In Fig. 6, we show evolution of the DOP of the RPGSMA beam at different values of coherence length δ_0 in free space. It can be found that, in the source plane, that the distribution of DOP of the RPGSMA beam is the same as that of a single conventional radially polarized beam, and related to the value of coherence length δ_0. Different coherence lengths result in different distributions of DOP. With an increase of the propagation distance, a periodical grid-like distribution in the central area appears, and the periodical distribution area gradually expands on propagation. This indicates that the RPGSMA beam gradually evolves into an array beams on propagation, and each single polarized beam in the array beams affects each other, resulting in a grid-like distribution of DOP of the RPGSMA beam.

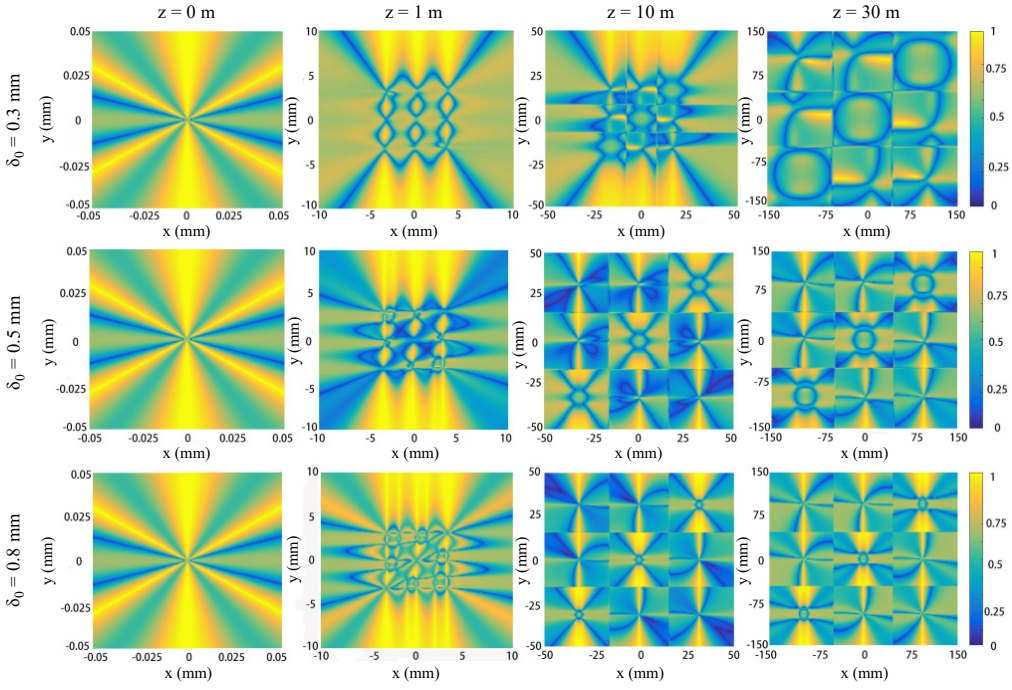

Fig. 6. Variation of DOP of the RPGSMA beam at different values of coherence length δ_0 in free space, and beam width w_0 = 1 mm.

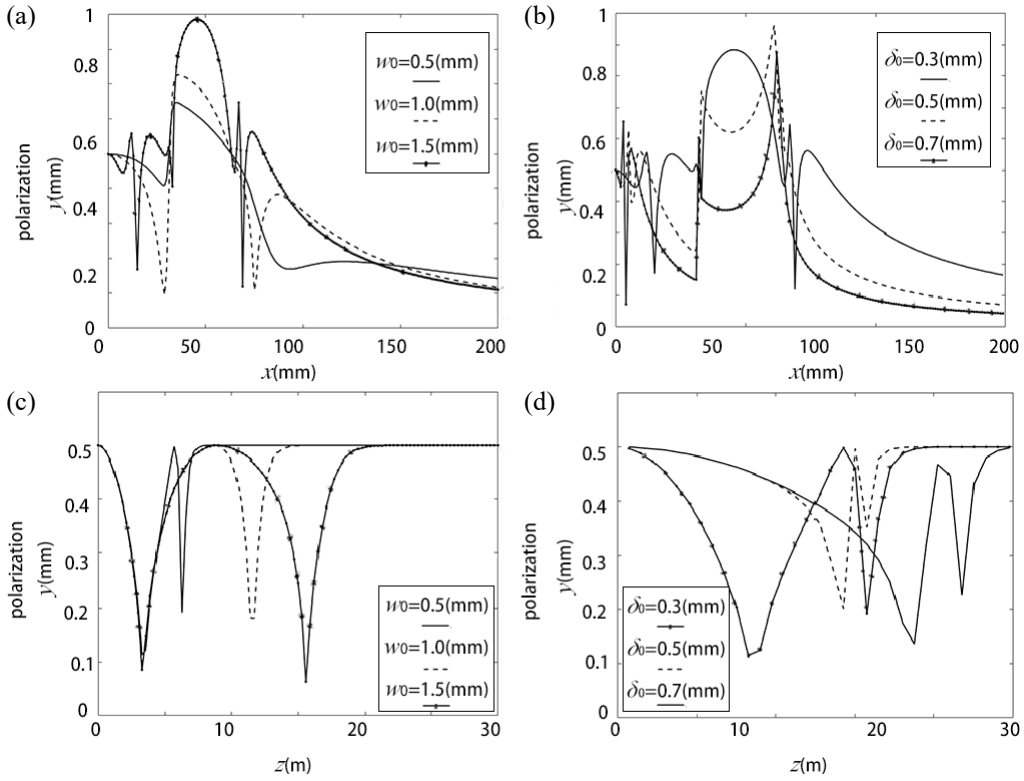

Fig. 7. Variation of polarization properties of the RPGSMA beam at different values of beam parameters in free space. (a), (b) Variation of DOP with the coordinate x at propagation distance z = 20 m. (c), (d) On-axis behaviors of DOP along propagation distance z. (a), (c), δ_0 = 0.3 mm, and (b), (d) w_0 = 0.5 mm

As shown in Fig. 7, variation of polarization properties of the RPGSMA beam at different values of beam parameters in free space has been further discussed. From Fig. 7(a) and (b), one can see that, in the cross-section, as the coordinate x increases, distribution of DOP of the RPGSMA beam initially fluctuates greatly, and then tends to be stable value. The smaller the beam width and coherence length, the larger the stable value. From Fig. 7(c) and (d), we also find that the on-axis behaviors of DOP show obvious fluctuations at first, and gradually became stable as the propagation distance increases. As the beam width and coherence length become larger, the on-axis DOP of the RPGSMA beam will get a stable value at a longer propagation distance.

5. Conclusion

In conclusion, we have introduced a new kind of partially coherent vector beam which can generate radially polarized Gaussian Schell-model array field, and discussed the reliability conditions. An analytical expression for the elements of the CSD matrix of a radially polarized Gaussian Schell-model array beam in free space is derived. With

the help of this formulae, the statistical properties of a RPGSMA beam on propagation have been studied numerically in detail. It is shown that the beam field generated by such a light source will produce far fields with optical lattice average intensity patterns. The DOC shows Gaussian profile in the far field, and the DOP appears a periodical grid-like distribution on propagation. In addition, It is also found that, with an appropriate choice of the source parameters and propagation distance, it can be a flexibly tuned propagation behavior of the RPGSMA beam. Our results might be beneficial for optical trapping, material processing, and free-space and atmospheric optical communications.

Funding
This study was funded by National Science Foundation of China (12265018).

Conflict of interest
The authors declare that they have no conflict of interest.

References

[1] ANDERSON B.P., GUSTAVSON T.L., KASEVICH M.A., *Atom trapping in nondissipative optical lattices*, Physical Review A **53**(6), 1996: R3727(R). https://doi.org/10.1103/PhysRevA.53.R3727
[2] OSTROVSKAYA E.A., KIVSHAR Y.S., *Photonic crystals for matter waves: Bose-Einstein condensates in optical lattices*, Optics Express **12**(1), 2004: 19-29. https://doi.org/10.1364/OPEX.12.000019
[3] MACDONALD M.P., SPALDING G.C., DHOLAKIA K., *Microfluidic sorting in an optical lattice*, Nature **426**, 2003: 421-424. https://doi.org/10.1038/nature02144
[4] YANG X.L., CAI L.Z., LIU Q., LIU H.-K., *Theoretical bandgap modeling of two-dimensional square photonic crystals fabricated by the interference of three noncoplanar laser beams*, Journal of the Optical Society of America B **21**(9), 2004: 1699-1702. https://doi.org/10.1364/JOSAB.21.001699
[5] MEI Z., ZHAO D., KOROTKVA O., MAO Y., *Gaussian Schell-model arrays*, Optics Letters **40**(23), 2015: 5662-5665. https://doi.org/10.1364/OL.40.005662
[6] EYYUBOĞLU H.T., BAYKAL Y., CAI Y., *Scintillation of laser array beams*, Applied Physics B **91**, 2008: 265–271. https://doi.org/10.1007/s00340-008-2966-x
[7] JI X., PU Z., *Angular spread of Gaussian Schell-model array beams propagating through atmospheric turbulence*, Applied Physics B **93**, 2008: 915–923. https://doi.org/10.1007/s00340-008-3256-3
[8] ZHOU P., MA Y.X., WANG X.L., MA H.T., XU X.J., LIU Z.J., *Average intensity of a partially coherent rectangular flat-topped laser array propagating in a turbulent atmosphere*, Applied Optics **48**(28), 2009: 5251-5258. https://doi.org/10.1364/AO.48.005251
[9] ZHOU P., WANG X.L., MA Y.X., MA H.T., XU X.J., LIU Z.J., *Propagation of partially coherent partially phase-locked laser array in turbulent atmosphere*, Optics Communications **283**(6), 2010: 1071-1074. https://doi.org/10.1016/j.optcom.2009.10.118
[10] ZHOU G.Q., *Propagation of a radial phased-locked Lorentz beam array in turbulent atmosphere*, Optics Express **19**(24), 2011: 24699-24711. https://doi.org/10.1364/OE.19.024699
[11] HUANG Y.P., HUANG P., WANG F.H., ZHAO G.P., ZENG A.P., *The influence of oceanic turbulence on the beam quality parameters of partially coherent Hermite–Gaussian linear array beams*, Optics Communications **336**, 2015: 146-152. https://doi.org/10.1016/j.optcom.2014.09.055
[12] WANG Y.K., MA H.X., ZHU L.H., TAI Y.P., LI X.Z., *Orientation-selective elliptic optical vortex array*, Applied Physics Letters **116**(1), 2020: 011101. https://doi.org/10.1063/1.5128040
[13] SHIRAI T., WOLF E., *Correlations between intensity fluctuations in stochastic electromagnetic beams of any state of coherence and polarization*, Optics Communications **272**(2), 2007: 289-292. https://doi.org/10.1016/j.optcom.2006.11.041

[14] XU J., ZHAO D., *Propagation of a stochastic electromagnetic vortex beam in the oceanic turbulence*, Optics & Laser Technology **57**, 2014: 189-193. https://doi.org/10.1016/j.optlastec.2013.10.019
[15] WOLF E., *Unified theory of coherence and polarization of random electromagnetic beams*, Physics Letters A **312**(5-6), 2003: 263-267. https://doi.org/10.1016/S0375-9601(03)00684-4
[16] DU X., ZHAO D., *Polarization modulation of stochastic electromagnetic beams on propagation through the turbulent atmosphere*, Optics Express **17**(6), 2009: 4257-4262. https://doi.org/10.1364/OE.17.004257
[17] ZHOU Y., ZHAO D., *Statistical properties of electromagnetic twisted Gaussian Schell-model array beams during propagation*, Optics Express **27**(14), 2019: 19624-19632. https://doi.org/10.1364/OE.27.019624
[18] ZHAN Q., *Cylindrical vector beams: from mathematical concepts to applications*, Advances in Optics and Photonics **1**(1), 2009: 1-57. https://doi.org/10.1364/AOP.1.000001
[19] FU W., ZHANG H., *Propagation properties of partially coherent radially polarized doughnut beam in turbulent ocean*, Optics Communications **304**, 2013: 11-18. https://doi.org/10.1016/j.optcom.2013.03.029
[20] WU G., WANG F., CAI Y., *Coherence and polarization properties of a radially polarized beam with variable spatial coherence*, Optics Express **20**(27), 2012: 28301–28318. https://doi.org/10.1364/OE.20.028301
[21] LIU D., WANG Y., ZHONG H., *Average intensity of radial phased-locked partially coherent standard Hermite-Gaussian beam in oceanic turbulence*, Optics & Laser Technology **106**, 2018: 495–505. https://doi.org/10.1016/j.optlastec.2018.05.015
[22] MEI Z., KOROTKOVA O., *Random sources for rotating spectral densities*, Optics Letters **42**(2), 2017: 255-258. https://doi.org/10.1364/OL.42.000255
[23] MEI Z., KOROTKOVA O., *Twisted EM beams with structured correlations*, Optics Letters **43**(16), 2018: 3905-3908. https://doi.org/10.1364/OL.43.003905
[24] GORI F., RAMÍREZ-SÁNCHEZ V., SANTARSIERO M., SHIRAI T., *On genuine cross-spectral density matrices*, Journal of Optics A: Pure and Applied Optics **11**(8), 2009: 085706. https://doi.org/10.1088/1464-4258/11/8/085706

Received November 7, 2022